

Influence of the Lattice Potential on the Line Shape of γ Rays Emitted by Sm Nuclei Recoiling with 3 eV in Eu Metal and EuO[†]

J. KALUS*

Bartol Research Foundation of the Franklin Institute, Swarthmore, Pennsylvania 19081

(Received 19 August 1969)

The change in velocity of the Sm¹⁵² nuclei recoiling with an initial energy of 3 eV after the electron-capture decay of Eu¹⁵², and thus the shapes of γ lines emitted after the neutrino emission, depend strongly on the source material. To scan these line shapes for polycrystalline Eu¹⁵² metal and Eu¹⁵²O sources, these sources were placed on the periphery of an ultracentrifuge, and the yields of resonantly scattered 963-keV γ rays were measured for different source velocities. In view of the low recoil energies involved and of the short lifetime of the nuclear state, the line shapes could be calculated to a good approximation by assuming that the recoiling nuclei were moving in a spherical potential. With EuO single-crystal sources, a small variation ($\sim 1\%$) of the nuclear resonance fluorescence (NRF) yield was observed for different orientations of the crystal relative to the Sm scatterer. From this, an estimate of the amount of anisotropy in the potential was deduced. As a byproduct of the ultracentrifuge measurements, the difference in energy between the ground state of Eu¹⁵² (9.3 h) and the 0.963-MeV level of Sm¹⁵² was determined to be 961.5 ± 5 keV, which is in agreement with other measurements.

I. INTRODUCTION

THE shapes of the γ lines emitted by recoiling nuclei depend, via the Doppler effect, on the change in velocity of the recoil. By scanning the line shape one can, therefore, obtain information about the time dependence of the recoil velocity.

In the usual NRF experiment, the photon intensity for a particular region of the emission line is determined, namely, for the region covered by the absorption line. If it is possible to shift the emission line relative to the absorption line in such an NRF experiment, one does, indeed, scan the shape of the emission line. In the special case of the 963-keV transition in Sm¹⁵², an ultracentrifuge permits one to perform such an experiment and scan an appreciable fraction of the emission line. Since the absorption line is about 1 eV wide, i.e., since it is an order of magnitude smaller than the width of the emission line, the analysis of such an experiment is rather straightforward.

The decay of Eu¹⁵² (9.3 h) to the 963-keV level of Sm¹⁵² provides a recoil energy of only 3 eV, and about 20 eV is necessary to remove an atom from the lattice position; the Sm nuclei can thus only oscillate around their mean positions.

As far as the calculation of the shape of the 963-keV emission line is concerned, an important simplification stems from the fact that the mean lifetime of 3.9×10^{-14} sec of the 963-keV level of Sm¹⁵² is considerably shorter than the oscillation time of the recoil in the lattice. The shape of the emission line reflects, therefore, only the decrease of velocity at the beginning of the damped oscillation of the recoil and can be deduced with a minimum number of adjustable parameters.

In the following sections we shall describe calculations of the shapes of the emission lines and of the corresponding NRF yields, describe the experimental

procedures, and analyze the data obtained with polycrystalline sources of Eu metal, EuO, and with a single crystal of EuO. From a comparison of the experimental NRF yields with the yields calculated for different decreases of velocity, conclusions concerning the forces acting on the Sm recoils are reached and relationships of these forces with the macroscopic behavior of Eu metal and EuO will be presented.

II. CALCULATION OF SHAPE OF EMISSION LINE

A. Initial Velocity Spectrum of Recoils

The first step for a calculation of the shape of the emission line is the determination of the velocity spectrum $H(V_0)$ of the nuclei at time $t=0$. At time $t=0$, Eu¹⁵² decays, via electron capture, by emission of a neutrino to the 963-keV level of Sm¹⁵² (Fig. 1), giving a recoil energy of 3 eV to the nucleus. Because of the creation of holes in the *K* and *L* shells and the subsequent emission of x rays and Auger electrons, the atom gains or loses additional, but much smaller, amounts of recoil energy. The characteristic time for the emission of the more energetic x rays and Auger electrons—and only these make an important contribution to the recoil energy—is in the region of 10^{-16} sec.¹ This time is short compared with the lifetime $\tau = 3.9 \times 10^{-14}$ sec² of the 963-keV level. Therefore, we assumed for the calculation that these processes also happen at time $t=0$. The data used for the transitions in the atomic shells can be found elsewhere.^{1,3,4} The velocity spectrum calculated in this manner shows a very complicated shape.

¹ M. A. Blochin, *Physik der Röntgenstrahlen* (Teubner, Leipzig, 1957).

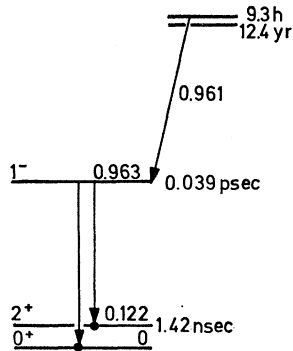
² F. R. Metzger, *Phys. Rev.* **B137**, 1415 (1965).

³ P. E. Zweifel, in *Proceedings of the Rehovoth Conference on Nuclear Structure*, edited by H. J. Lipkin (North-Holland, Amsterdam, 1965), p. 300 ff.

⁴ I. Bergström and C. Nordling, in *Alpha-, Beta-, and Gamma-Ray Spectroscopy*, edited by K. Siegbahn (North-Holland, Amsterdam, 1965).

[†] Supported in part by the U. S. Atomic Energy Commission.

* Permanent address: Physik Department der Technischen Hochschule München, Germany.

FIG. 1. Partial decay scheme of Eu^{152} .

By including, as is usually done, a Maxwellian distribution for the thermal velocity of the atoms,⁵ the shape is smoothed out and looks approximately like a Gaussian curve with its center at a velocity of 1.96×10^5 cm/sec and with a half-width of 3.28×10^4 cm/sec for an effective temperature of 320°K .

B. Change in Velocity of the Recoils in a Polycrystal

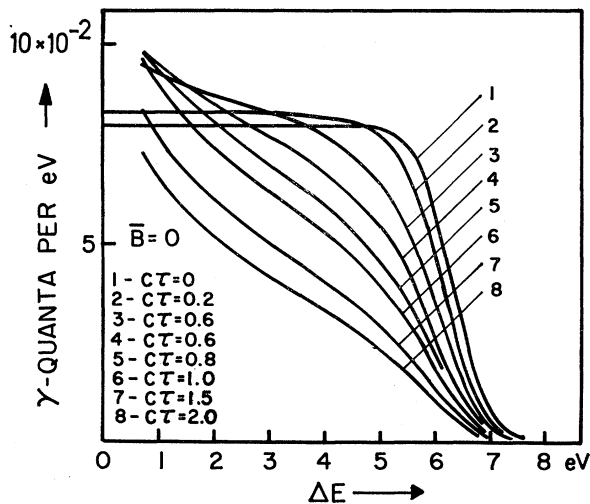
For the calculation of the change in velocity of the recoils the following assumptions were made:

(1) At time $t=0$, the Sm recoils are at the mean lattice positions of the Eu atoms. Neglecting the influence of the lattice vibrations on the initial positions of the recoils gives only an error of second order in the shape of the emission line.

(2) The recoils move in a potential of the form

$$P = \frac{1}{2}MC^2[r^2 + B(\alpha)r^4], \quad (1)$$

where M is the mass of the recoil, r is the distance of the recoil from the mean position, and B and C are param-

FIG. 2. Calculated shapes of the 0.963-MeV emission line for $\bar{B}=0$ and for different values of the potential parameter $C\tau$.

⁵ W. E. Lamb, Phys. Rev. **55**, 190 (1939).

eters, to be adjusted. Higher orders in r are neglected. In a cubic crystal only B , and not C , depends on the direction α in the crystal. But with polycrystalline sources, one can gain only information about a mean value of $B(\alpha)$, for which we introduce the symbol \bar{B} .

(3) The velocity $V(t)$ can be restricted as follows: (a) If $V(t)=0.01 V(0)$ for $t=t'$, $V(t)$ for $t>t'$ is assumed to be of the form $V(t)=0.01 V(0) \exp(-\lambda t)$ with $\lambda \ll 1/\tau$. (b) If $(dV/dt)=0$ for $t=t''$ ($t'' \neq 0$), $V(t)$ for $t>t''$ is assumed to be of the form $V(t)=V(t'') \exp(-\lambda t)$ with $\lambda \ll 1/\tau$.

These simplifications do not have a significant influence in the restricted region of the emission line we could measure, because t' and t'' for reasonable values of the parameters C and \bar{B} are larger than the lifetime τ of the 963-keV level in Sm^{152} . The conditions (a) and (b) are useful because $V(t)$ is then always positive, single-valued, and time-dependent. The value of the arbitrarily introduced parameter λ is not critical.

C. Shape of the Emission Line

The shape of the emission line as a function of the energy, $N(|\Delta E|, C, \bar{B})$, is given by the following expression⁶:

$$N(|\Delta E|, C, \bar{B}) = \text{const} \int_0^\infty H(V_0) \times \int_0^T e^{-t/\tau} [\tau V(t)]^{-1} dt dV_0, \quad (2)$$

with $V(0)=V_0$ and $\Delta E = E_\gamma - E_0 + E_0^2/2Mc^2$, where E_γ is the energy of the emitted γ ray, E_0 is the energy of the excited state, and c is the velocity of light. The upper limit T for the integration is zero for $V(0) E_0/c < \Delta E$; otherwise one has to solve the equation $V(T) E_0/c = \Delta E$. $N(|\Delta E|, C, \bar{B})$ is symmetrical about $\Delta E=0$. Figures 2 and 3 show results of the calculations for different parameters C and \bar{B} .

III. CALCULATION OF THE NRF YIELD

A. NRF Yield for the Polycrystalline Sources

The NRF yield in a scattering experiment (Fig. 4) for a thin scatterer is given by⁷

$$Z(\Delta E_0, C, \bar{B}) = \text{const} \int_0^\infty N(|\Delta E|, C, \bar{B}) \sigma(\Delta E, \Delta E_0) d(\Delta E), \quad (3)$$

where ΔE_0 is the difference in energy between the centers of the emission line and the absorption line. If the entire source is moved towards the scatterer with a

⁶ J. B. Cumming, A. Schwarzschild, A. W. Sunyar, and N. T. Porile, Phys. Rev. **120**, 2128 (1960).

⁷ F. R. Metzger, Progr. Nucl. Phys. **7**, 53 (1959).

velocity W , then ΔE_0 is given by

$$\Delta E_0 = E_0^2/Mc^2 - WE_0/c. \quad (4)$$

The shape of the absorption line, $\sigma(\Delta E, \Delta E_0)$, is well known.⁷

The scatterer used in our experiment could not be treated as thin, and this was taken into account in the evaluation of the data. For a discussion of this problem, see Ref. 7.

B. NRF Yield for a Single-Crystal Source

For a single crystal, B in Eq. (1) becomes dependent on the direction α in the crystal. Since the accuracy of the anisotropy measurement was rather poor, only a first-order correction to Eq. (3) was applied in the calculation of the anisotropic NRF yields. We neglected the fact that the path of the recoils is no longer straight. The effect of deviations from the straight line on the NRF yield has been discussed by Abel.⁸ For further discussion of the NRF yield for a single crystal, it is convenient to introduce two angular functions $F(\nu)$ and $\Delta B(\nu)$:

$$Z(\nu, \Delta E_0, C, B) = Z(\Delta E_0, C, \bar{B}) [1 + F(\nu)] \quad (5)$$

with $F(\nu) \ll 1$,

$$B(\alpha) = \bar{B} + \Delta B(\alpha). \quad (6)$$

ν defines the orientation of the single crystal relative to the direction single-crystal-scatterer, and α defines a direction in the single crystal. It is not necessary that $\Delta B(\alpha) < \bar{B}$. A calculation of the relative contribution $y(\beta)$ of a nucleus recoiling in direction β to the total NRF yield, where β is the angle between the direction of flight of the recoil and the direction source-scatterer, gives the result that $y(\beta)$ is peaked around $\beta=0$ and vanishes for $\beta \gtrsim 36^\circ$, provided the source velocity W is zero or small.⁹ We can write

$$Z(\nu, \Delta E_0, C, B) \simeq \int \left\{ Z(\Delta E_0, C, \bar{B}) + \left(\frac{dZ(\Delta E_0, C, \bar{B})}{d\bar{B}} \right) \times \Delta B(\beta) \right\} y(\beta) d\Omega / \int y(\beta) d\Omega, \quad (7a)$$

$$F(\nu) \simeq \int \left(\frac{dZ(\Delta E_0, C, \bar{B})}{d\bar{B}} \right) \Delta B(\beta) y(\beta) d\Omega / \left\{ Z(\Delta E_0, C, \bar{B}) \int y(\beta) d\Omega \right\}, \quad (7b)$$

where $d\Omega$ is an element of solid angle. Equations 7(a) and 7(b) are exact within the limits of the theory if ΔB is independent of β , or if $y(\beta) = \delta(\beta)$. The latter case is

⁸ F. Abel, Dissertation at Technische Hochschule München, 1968 (unpublished).

⁹ F. Abel and J. Kalus, Phys. Status Solidi 32, 619 (1969).

fairly well realized if the source velocity W is zero or small. Equation (7) normally is only an approximation, because we neglected that $y(\beta)$ could also depend on B .

IV. EXPERIMENTAL PROCEDURES

A. Experiments with Polycrystalline Source of Eu metal and EuO

The velocity W of the sources was achieved by placing them on the periphery of a titanium-alloy rotor in a conventional scattering geometry (Fig. 4). The samarium metal scatterer measured $0.87 \times 3.85 \times 5.85$ cm. Neodymium metal served as the comparison scatterer. Sources of 1 Ci of 9.3-h Eu^{152} , prepared by neutron irradiation of Eu metal and EuO, were used. Because Eu metal and EuO are subject to corrosion in humid air, they were sealed, in an inert argon-gas atmosphere, into small steel tubes.

The output of the 3×3 -in. NaI(Tl) detector system was connected to a 400-channel RIDL analyzer. A lead absorber, 0.8 cm thick, placed in front of the detector, removed the intense low-energy background component from the scattered radiation. Measurements were carried out for source velocities of up to 10^6 cm/sec. A typical pulse-height distribution is shown in Fig. 5.

B. Experiments with EuO Single Crystals

Preliminary experiments showed that the NRF anisotropy is very small and therefore indicated that the accuracy of the measurements had to be in the region of 0.1%. The change in orientation was achieved^{9,10} by placing the EuO single crystal into a tube which could be rotated around its cylindrical axis once a second. The [001] direction of the crystal (NaCl structure) was made to coincide with the axis of the tube. This axis

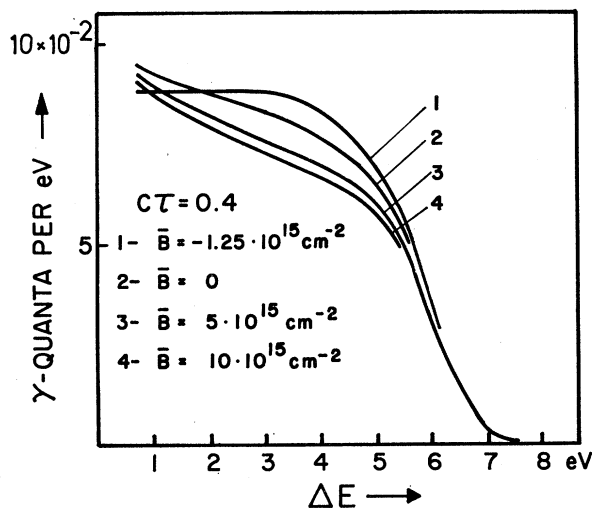


FIG. 3. Calculated shapes of the 0.963-MeV emission line for $C\tau=0.4$ and for different values of the potential parameter \bar{B} .

¹⁰ J. Kalus and H. J. Thaler, Z. Naturforsch. 23a, 283 (1968).

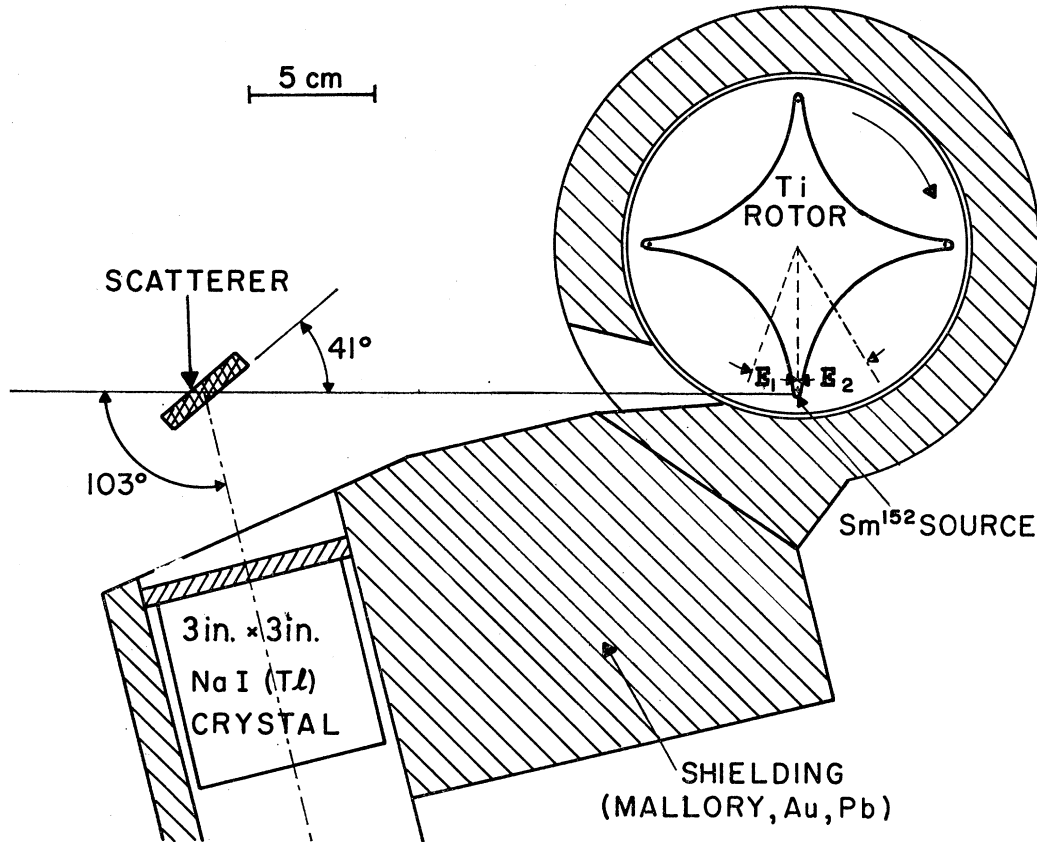


FIG. 4. Experimental arrangement for the scattering experiment with the centrifuge.

was perpendicular to the plane containing the source, the scatterer, and the NaI detector. The output of the NaI detector was connected to two single-channel analyzers; one accepted pulses in the region of the resonance line, the other in the region of the Compton-scattered γ quanta. The intensity of the Compton-scattered γ quanta was at least one order of magnitude higher, and therefore the influence of pulses connected with resonant events was negligible. A disk with 100 identical slots on its periphery was mounted with the tube as its axle. A light beam, interrupted 100 times for every revolution of the disk, provided signals for the multiscaler mode of the RIDL analyzer. A switching mechanism fed the resonant events into the first 100 channels of the multiscaler, and the nonresonant events, which were used for the calibration of the first 100 channels, into the second 100 channels. Therefore, neglecting the averaging over 3.6° , the counting rate in each channel was accumulated for a distinct orientation of the single crystal. The calibration by means of the nonresonant events gives an automatic correction to the counting rate of the resonant events if the solid angle between source and scatterer is subject to periodic changes. Such changes occur, when the center of the crystal does not coincide with the axis of the tube. The system was very insensitive to changes in the electronics

and in the rotation frequency. Tests proved that an accuracy of at least 0.1% is normal.

V. ANALYSIS OF THE EXPERIMENTAL DATA

A. Polycrystalline Sources of Eu Metal and EuO

The relative resonance yields, measured in the scattering experiments for different rotor speeds, i.e., as a function of the energy separation ΔE_0 of the centers of the emission and absorption lines, are plotted in Fig. 6. The yields are plotted at the abscissas corresponding to the respective tangential source velocities, although, as indicated in Fig. 4, the measurements as well as the calculations are averaged over emission angles E_1 and E_2 differing by as much as 20° and 30° from the tangential direction.

In evaluating the information of the time dependence of the recoil velocity contained in Fig. 6, we made a least-squares fit, using Eq. (3) with C and \bar{B} as parameters. Values at energies higher than $\Delta E_0 = 6.30$ eV were excluded from the fitting procedure, because this region is sensitive to the not exactly known decay processes in the atomic shell. The results of the calculations are presented for Eu metal and EuO in Fig. 7. In addition to this information which depends only on the shapes of the relative yield curves, further restrictions on the

parameters C and \bar{B} describing the potential are obtained from a comparison of the measured absolute yields expected on the basis of the known width of the level. To determine the absolute yields, the scattering geometry had to be calculated, taking into account, among other effects, the self-absorption in the thick scatterer, the electronic attenuation of the incident and outgoing radiation, the angular distribution of the resonant radiation, and the branching² from the 963-keV level. The transition energy of the electron capture to the 963-keV level in Sm^{152} was assumed to be 960 keV. Included in Fig. 7 are the results from this evaluation, assuming an over-all error of 13% for the calculation of the absolute yields.

Improvements in the determination of C and \bar{B} are still possible, either by a more accurate determination of the absolute NRF yield, which is equivalent to a measurement of the lifetime τ with the same precision, or by the development of a rotor with a tangential velocity of 2 km/sec. In the latter case, it would be possible to determine the resonance-effect-versus- ΔE_0 curve down to $\Delta E_0=0$ and thus to be in a position to normalize the experimental points properly.

B. EuO Single-Crystal Source

Because of the special orientation of the single crystal, described in Sec. IV, the orientation ν of the crystal with respect to the direction crystal-scatterer can be described by a single angle ν' , and the related counting

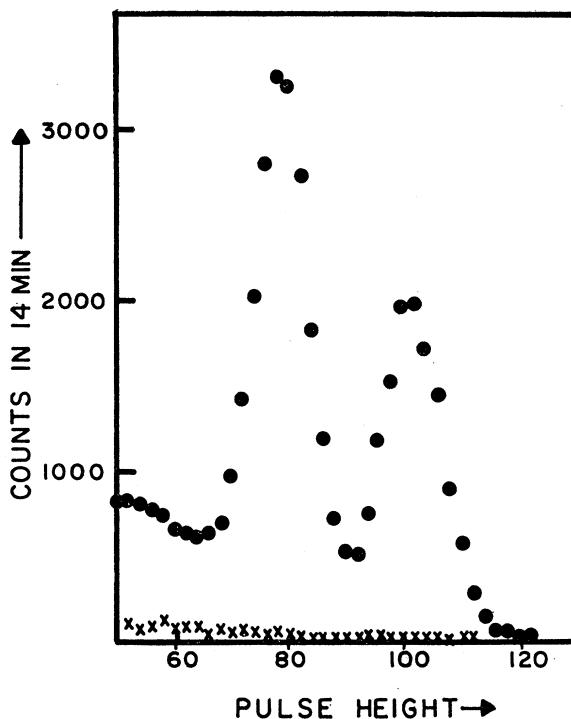


FIG. 5. Resonance scattering from Sm (\bullet) at a source velocity of 8.5×10^4 cm/sec. The pulse-height distribution exhibits two peaks, since the 0.963-MeV level decays to the 0.122-MeV level as well as to the ground state. The background (\times) was measured with a Nd scatterer.

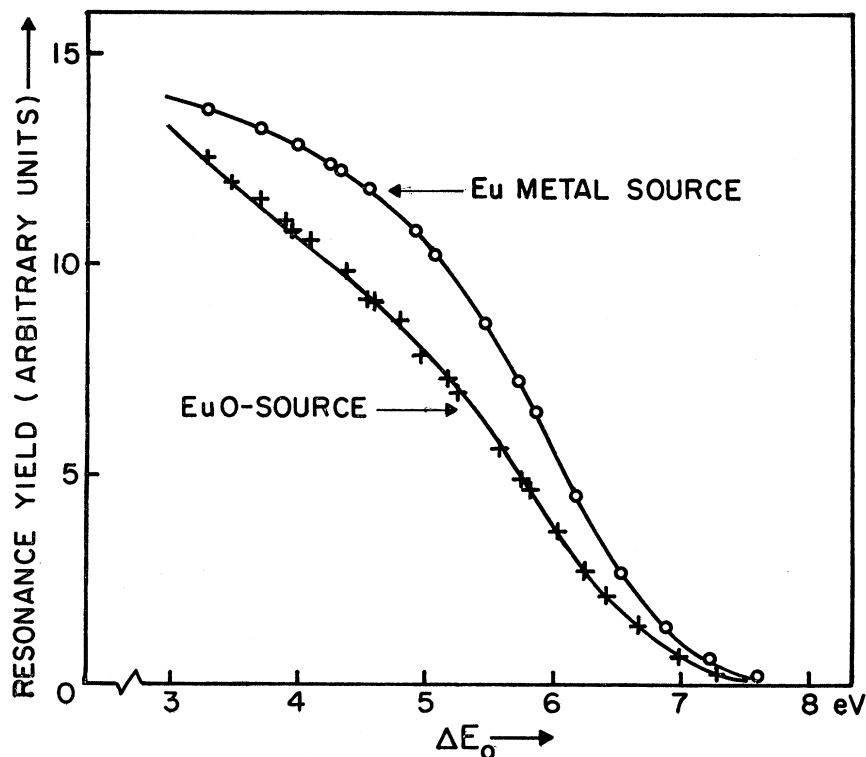


FIG. 6. Resonance scattering from the 0.963-MeV level for different source velocities, corresponding to separations ΔE_0 of the absorption line from the center of the emission line, for an Eu-metal source (\circ) and an EuO source ($+$). The smooth curves were calculated with $C\tau=0.4$, $\bar{B}=0$ for Eu metal and $C\tau=0.8$, $B=-0.25 \cdot 10^{16}$ cm⁻² for EuO. The ratio of the measured yields for Eu metal and EuO at $\Delta E_0=3.3$ eV is $Z(\text{Eu})/Z(\text{EuO})=1.095 \pm 0.02$. The over-all errors in the resonance yields below $\Delta E_0=6.25$ eV are 1% for Eu metal and 1.5% for EuO.

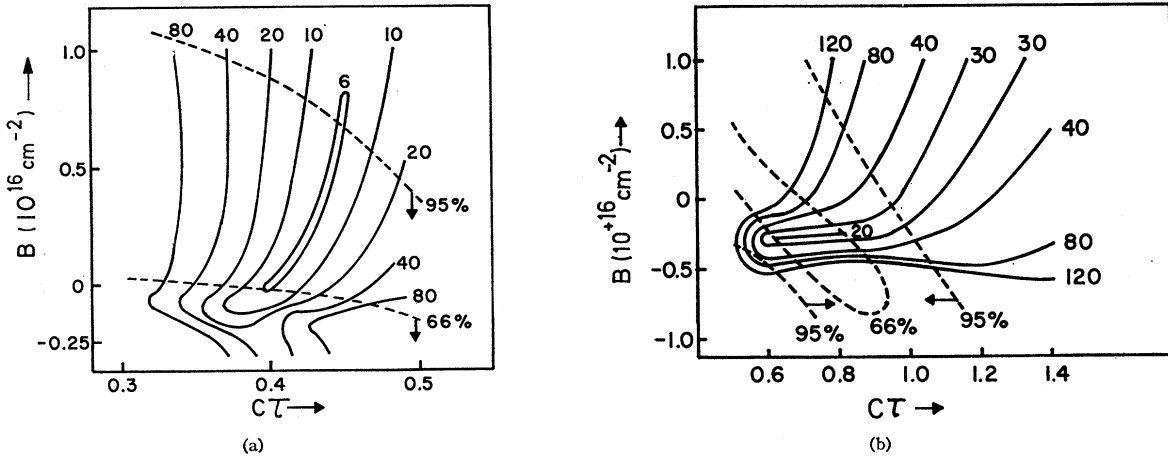


FIG. 7. (a) Results of the least-squares-fit calculation, using the potential from Eq. (1), for Eu metal (solid lines). The figures on the curves are the values of χ^2 in the \bar{B} - $C\tau$ plane. The dashed lines represent the limits imposed on \bar{B} and $C\tau$, based on a determination of the absolute yield. The figures on these lines give the probability that \bar{B} and $C\tau$ are in the region indicated by the arrows. (b) Results of the least-squares-fit calculation, using the potential from Eq. (1), for EuO (solid lines). The figures on the curves are the values of χ^2 in the \bar{B} - $C\tau$ plane. The dashed lines represent the limits imposed on \bar{B} and $C\tau$, based on a determination of the absolute yield. The figures on these lines give the probability that \bar{B} and $C\tau$ are in the region indicated by the arrows.

rates of resonant events in an angular interval $\nu_1' - \nu_2'$ by $Z(\nu_1' - \nu_2')$. Let us choose $\nu' = 0$ if the [100] direction of the crystal coincides with the direction single-crystal-scatterer; then the results of the measurement are

$$\frac{Z(22.5^\circ - 45^\circ)}{Z(0^\circ - 22.5^\circ)} = 1.0068 \pm 0.0017. \quad (8)$$

The special orientation allows one to represent $Z(\nu')$ in first order by a function

$$Z(\nu') \approx Z(\Delta E_0, C, \bar{B})(1 - a \cos 4\nu') \quad (9)$$

with

$$a = 0.0053 \pm 0.0013. \quad (10)$$

It is impossible to obtain detailed information concerning $\Delta B(\alpha)$ [see Eq. (6)] from this measurement. To do that, one would have to determine $Z(\nu)$ for all orientations ν .

We used two models for an estimate of the magnitude of $\Delta B(\alpha)$:

$$(1) \quad B = \bar{B} + \Delta B(\alpha) = \bar{B} + \Delta B_1 \cos(4\alpha'). \quad (11)$$

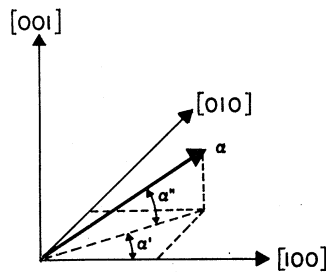


FIG. 8. Definition of the angles α' and α'' introduced in Eqs. (11) and (12).

This is a two-dimensional model which underestimates $\Delta B(\alpha)$.

$$(2) \quad B = \bar{B} + \Delta B(\alpha) = B + \Delta B_2 \cos(4\alpha') \cos(4\alpha''). \quad (12)$$

This model gives a relatively good approximation to the true $\Delta B(\alpha)$ near $\alpha' = 0^\circ$ and 45° . The angles α' and α'' are defined in Fig. 8. Using Eq. (6) and Eq. (7), one obtains in first order

$$\Delta B_\epsilon \approx aZ(\Delta E_0, C, \bar{B})F_\nu \left/ \left[\frac{dZ}{dB} \right] \right., \quad \epsilon = 1, 2 \quad (13)$$

$$F_1 = 2.4, \quad F_2 = 3.3. \quad (14)$$

The function $Z(\Delta E_0, C, \bar{B})$ is shown in Fig. 9 for several values of the parameter C .

C. Difference in Energy between Ground State of Eu^{152} (9.3 h) and the 963-keV Level in Sm^{152}

The width of the emission line depends on the energy of the neutrino emitted in the decay of Eu^{152} (9.3 h) to the 963-keV level of Sm^{152} . A least-squares fit, including the information of the time dependence of the recoil velocity, gave for the energy E_{ec} between the ground state of Eu^{152} (9.3 h) and the 963-keV level of Sm^{152}

$$E_{ec} = 960 \pm 6 \text{ keV} \quad \text{for Eu metal}, \quad (15a)$$

$$E_{ec} = 965 \pm 8 \text{ keV} \quad \text{for EuO}. \quad (15b)$$

The weighted mean value of E_{ec} is 961.5 ± 5 keV. This value is in agreement with measurements made by Alburger *et al.*¹¹ and Antonova *et al.*¹² ($E_{ec} = 956 \pm 10$

¹¹ D. E. Alburger, S. Ofer, and M. Goldhaber, *Phys. Rev.* **112**, 1998 (1958).

¹² S. F. Antonova, S. S. Vasilenko, M. G. Kaganskij, and D. L. Kaminski, *Zh. Eksperim. i Teor. Fiz.* **37**, 667 (1959) [*Soviet Phys. JETP* **10**, 477 (1960)].

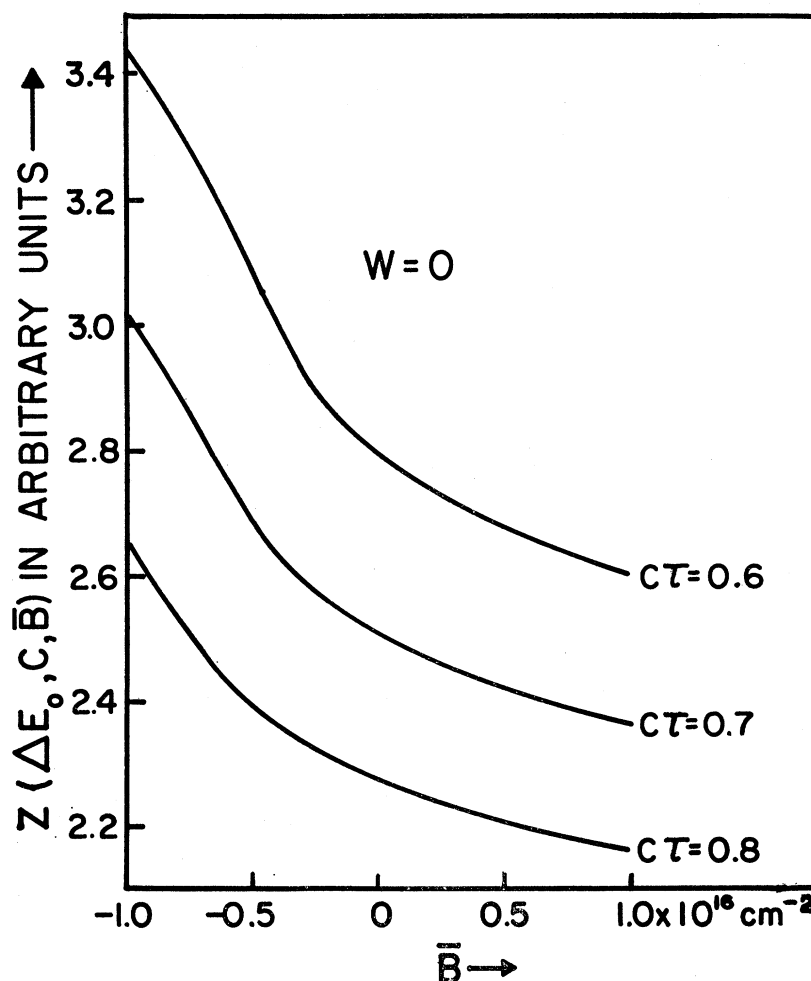


FIG. 9. Calculated dependence on \bar{B} of the resonance yield with a stationary Eu^{152} source, for different values of the parameter $C\tau$.

keV) with magnetic spectrometers, but not with measurements made by Kalus and Lades¹³ ($E_{ec}=946\pm 5$ keV) and Moon *et al.*¹⁴ ($E_{ec}=925\pm 10$ keV) with the NRF method. These authors made measurements in the region near the edge of the emission line, avoided in the determination presented here; consequently their results were sensitive to the decays in the atomic shells. It is then quite probable that a systematic error occurs.

VI. DISCUSSION

The potential P introduced in Sec. II has a close connection with the potential P' seen by a Sm atom moving in a hypothetical lattice, where all the other atoms have an infinite mass. The reason for this is the short lifetime τ of the excited state. During this short lifetime the neighbors of the Sm recoil in the real lattice do not have enough time to respond to the forces acting on them. We can therefore write $P' \simeq P$. This relation-

ship certainly holds true for Eu metal with its small value of the parameter C , but is also expected to be adequate for EuO.

The near equality of P' with P justifies the omission of a r^3 term in the potential, since this term in a cubic crystal is identically zero for the potential P' , if only central forces are considered.

Because we measured the decrease of velocity of a Sm atom in Eu and EuO hosts, it is difficult to find connections between the potentials deduced from these experiments and the macroscopic behavior of these materials. The estimates which follow should be judged with this in mind.

A. Eu Metal

If a central-force interaction with the nearest neighbors only is assumed, the parameter C is related to the compressibility κ as follows:

$$C \simeq 2(d/\kappa M)^{1/2}, \quad (16)$$

where d is the lattice constant. Inserting the values of κ

¹³ J. Kalus and H. Lades, *Z. Physik* **192**, 129 (1966).

¹⁴ P. B. Moon, G. G. Shute, and B. S. Sood, *Phys. Rev. Letters* **1**, 21 (1958).

and d for Eu and Sm metal, respectively,¹⁵⁻¹⁷ one finds

$$C\tau \simeq 0.38 \quad \text{for Eu metal} \quad (17)$$

and

$$C\tau \simeq 0.53 \quad \text{for Sm metal.}$$

The first value agrees rather closely with the result of the NRF experiment.

The characteristic frequency of the recoil, easy to calculate using Eq. (1) for $\bar{B}=0$, corresponds to an Einstein temperature of 80°K or a Debye temperature of $\simeq 110^\circ\text{K}$.¹⁸ This Debye temperature should be compared with the values of 107°K for Eu¹⁹ and 140°K for Sm metal.²⁰

The following information about \bar{B} is available:

(1) From a study of the anharmonic effects in fcc crystals²¹ with central forces between nearest neighbors, it can be concluded that \bar{B} must be negative.

(2) One obtains a crude estimate of the magnitude of \bar{B} by using Eq. (83.7) of Leibfried,²¹ which gives a value of \bar{B} of the order of $-3 \times 10^{15} \text{ cm}^{-2}$. But this value is only approximately valid for fcc crystals and therefore doubtful for the bcc lattice of Eu metal. After an examination of the results of the least-squares fit procedures, carried out in Sec. V, \bar{B} could be positive, but these theoretical considerations reduce this possibility.

¹⁵ A. M. Burkhanov, N. P. Grazhdankina, and I. G. Fakidov, *Fiz. Tverd. Tela* **9**, 748 (1967) [*Soviet Phys. Solid State* **9**, 586 (1967)].

¹⁶ P. W. Bridgman, *Proc. Am. Acad. Arts Sci.* **83**, 1 (1954).

¹⁷ A. H. Daane, in *The Rare Earths*, edited by F. H. Spedding and A. H. Daane (Wiley, New York, 1961), p. 177 ff.

¹⁸ M. Born and K. Huang, *Dynamical Theory of Crystal Lattices* (Clarendon, Oxford, 1956), p. 43.

¹⁹ B. C. Gerstein, F. J. Jelinek, J. R. Mullaly, W. D. Shickell, and F. H. Spedding, *J. Chem. Phys.* **47**, 5194 (1967).

²⁰ L. D. Jennings, E. D. Hill, and F. H. Spedding, *J. Chem. Phys.* **31**, 1240 (1959).

²¹ G. Leibfried, in *Handbuch der Physik*, edited by S. Flügge (Springer-Verlag, Heidelberg, 1955), Vol. VII, Part I, p. 104 ff.

B. EuO

With the restrictions mentioned above under (2), the variation of B in a EuO single crystal is expected to be $|\Delta B| \approx 2.5 \times 10^{15} \text{ cm}^{-2}$. This should be compared with a value of approximately $4.5 \times 10^{15} \text{ cm}^{-2}$ obtained from the experimental data using Eq. (13) and Eq. (14) for $\bar{B} = -0.25 \times 10^{16} \text{ cm}^2$, $C\tau = 0$, 8 and $F_2 = 3.3$.

Because of the transitions in the atomic shells of the recoiling Sm atoms, caused by the creation of an electron hole in the K or L shells, the binding of these Sm atoms in a crystal is disturbed. This is perhaps not so important in a metal where there are many conduction electrons available, but is surely important in an insulator such as EuO. The potential seen by the Sm recoil can thus differ from that seen by a normal Sm atom. Nevertheless, the method described here still allows the measurement of an effective anisotropic potential, and is sensitive to small changes—equivalent to a change of 2% in the parameter C —in the nearest neighborhood of a Sm recoil.

The variation of the NRF yield in a noncubic single crystal for different orientations can be several percent and therefore is easy to measure.⁹ An analysis of such a measurement provides information about the variation of the parameter C , which in these crystals is not a constant, but depends on the direction. The variation of the NRF yield in a cubic single crystal, where C is independent of the direction, is much smaller and therefore harder to measure, but the measurement now provides information about the variation of the anharmonic term B for different directions in the crystal.

ACKNOWLEDGMENTS

The author is grateful to Dr. F. R. Metzger for his helpful suggestions and wishes to express his appreciation to Professor G. Busch, Eidgenössische Technische Hochschule Zürich, for making the EuO single crystal available.